Three-dimensional runup simulation of the 2004 Indian Ocean tsunami at the Lhok Nga twin peaks

Dong Chule Kim†, Kyeong Ok Kim‡, Byung Ho Choi∞, Kyung Hwan Kim§, Efim Pelinovsky+

† Technology R&D Institute
Hyein E&C Co., Ltd., Seoul 157-861, Korea
skkkdc@chol.com

‡ Marine Environments & Conservation Research Division, Korea Institute of Ocean Science & Technology, Ansan 426-744, Korea
kokim@kiost.ac

∞ Dept. of Civil and Env. Engineering
Sungkyunkwan University, Suwon 440-746, Korea
bhchoi.skku@gmail.com
*corresponding author

§ Dept. of Engineering
STI C&D Co., Ltd., Seoul 153-786, Korea
hydro@stikorea.co.kr

+ Nizhny Novgorod State Technical University and Institute of Applied Physics, Nizhny Novgorod, Russia
pelinovsky@hydro.appl.sci-nnov.ru

www.cerf-jcr.org

www.JCRonline.org

ABSTRACT

Kim, D.C., Kim, K.O., Choi, B.H., Kim K.H. and Pelinovsky, E., 2013. Three-dimensional runup simulation of the 2004 Indian Ocean tsunami at the Lhok Nga twin peaks. *In:* Conley, D.C., Masselink, G., Russell, P.E. and O'Hare, T.J. (eds.), *Proceedings 12th International Coastal Symposium* (Plymouth, England), *Journal of Coastal Research*, Special Issue No. 65, pp. 272-277, ISSN 0749-0208.

A post-tsunami runup survey for the 2004 Sumatra–Andaman earthquake showed that the highest runup which was recorded at Lhok Nga (West Banda Aceh, Sumatra). A reported maximum tsunami height of 35 m and maximum runup height of up to 51 m occurred near the Lhok Nga Twin Peaks (Labuhan and Ritieng). A numerical simulation was performed to reproduce tsunami characteristics in this area. The tsunami source was computed using fault parameters proposed by Tanioka et al. Tsunami wave propagation from the source to the coast was studied with 3D shallow-water equations. The coastal runup behavior of the tsunami at the Lhok Nga Twin Peaks was studied within a framework of fully nonlinear dispersive Reynolds-averaged Navier–Stokes equations using the FLOW3D code. This approach made it possible to reproduce the extreme characteristics of the tsunami in this coastal area, including observed overflow through a saddleback between the twin peaks. The numerical simulation results compare well with data from field surveys.

ADDITIONAL INDEX WORDS: *Tsunami, shallow-water theory, Reynolds-Averaged Navier-Stokes equations*

INTRODUCTION

The tsunami that occurred in the Indian Ocean after the catastrophic Sumatra–Andaman earthquake on December 26, 2004 (magnitude Mw=9.3) was the strongest tsunami recorded in this century. It caused significant damage to coastal areas of the Indian Ocean and killed over 230,000 people (Lay et al., 2005; Satake et al., 2007). Tsunami waves were recorded by a large number of tide gauges throughout the world's oceans, including near-source regions of the Indian Ocean (Merrifield et al., 2005; Rabinovich and Thomson, 2007) and remote regions of the Pacific and Atlantic oceans (Titov et al., 2005; Rabinovich et al., 2006; Thomson et al., 2007; Candella et al., 2008). The event was absolutely unprecedented (Titov et al., 2005; Geist et al., 2006).

A post-tsunami runup survey of the 2004 Sumatra–Andaman earthquake (Lavigne et al., 2009; Paris et al., 2009) showed that the highest runup was recorded at the Leupung Beach Twin Peaks in Lhok Nga (Figure 1). The arrow in Figure 1 displays the direction of the tsunami wave, which crossed over the pass between Labuhan Hill and Ritieng Hill. The runup height of 51 m above sea level, measured on a cliff near Leupung on the west coast, is the highest recorded runup in human history for a seismically generated tsunami. It is important to mention other characteristics of the tsunami in this area observed during the field survey. In particular, the tsunami comprised approximately ten separate waves. There were also significant discontinuities in the tsunami wave heights and flow depths along a line approximately 3 km inland, which is interpreted as a collapse of the main tsunami bore caused by sudden energy dissipation. The propagating bore looked like a breaking wave, and the landward patterns of building damage were related to the location of the propagating bore, with less damage overall to buildings beyond the line where the bore collapsed. As underlined in (Lavigne et al., 2009), the data for this tsunami are very useful for calibrating and improving existing tsunami inundation models, especially in the analysis of extreme near-field events.

In this study, we attempted to reproduce the tsunami wave characteristics in the Lhok Nga area, including the extreme runup height and overflow of the saddleback between Labuhan Hill and Ritieng Hill. The wave field in the coastal area was modeled within the framework of fully nonlinear dispersive Reynolds-averaged Navier–Stokes (RANS) equations solved using the FLOW3D code. Boundary conditions for this model were extracted from computed wave characteristics obtained from the tsunami propagation model based on the Princeton Ocean Model (POM). The numerical simulation results compare well with the observed tsunami wave characteristics.

2004 SUMATRA-ANDAMAN TSUNAMI SOURCE

The issue of the best source model for the Sumatra 2004 earthquake for use in simulating consecutive tsunami is discussed

DOI: 10.2112/SI65-047.1 received 07 December 2012; accepted 06 March 2013.

in the literature (Poisson et al., 2011). In our computations, we used the fault parameters proposed by Tanioka et al. (2006) to estimate the rupture process of the 2004 Sumatra–Andaman earthquake. The largest slip, 23 m, is estimated to have occurred off the northwest coast of the Aceh Province of Sumatra in Indonesia. Four fault models were considered, and the results of Model B, for which the average rupture speed was 1.7 km/s, yielded the best fit with observations from tide gauges. In this study, the modified fault parameters of the Sumatra–Andaman earthquake, based on Model B, were used (Table 1) with the rake angle fixed at 90 degrees. The locations are the southwest corners of each subfault and the depth is the top edge.

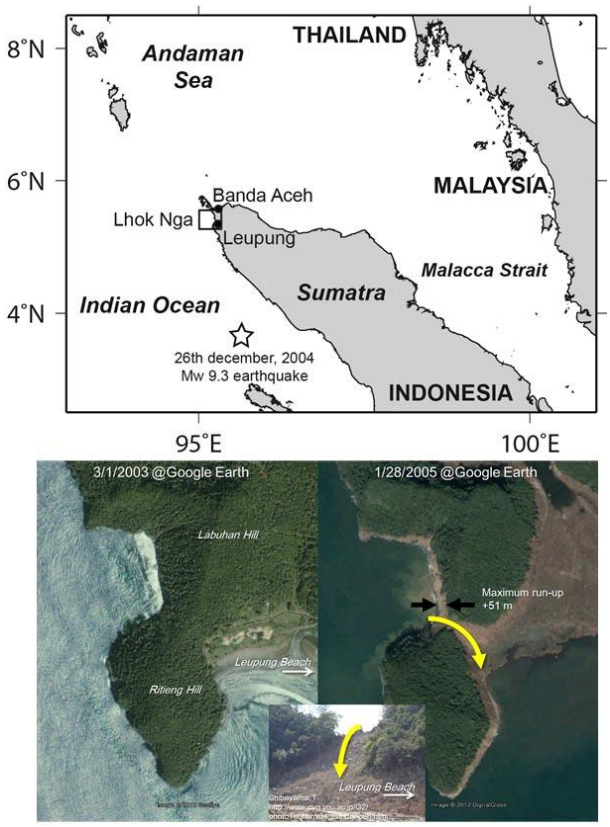

Figure 1. The location of Lhok Nga and the runup height of 51 m measured on a cliff near Leupung, on the west coast. The arrow displays the direction of the tsunami wave, which crossed the pass between Labuhan Hill and Ritieng Hill.

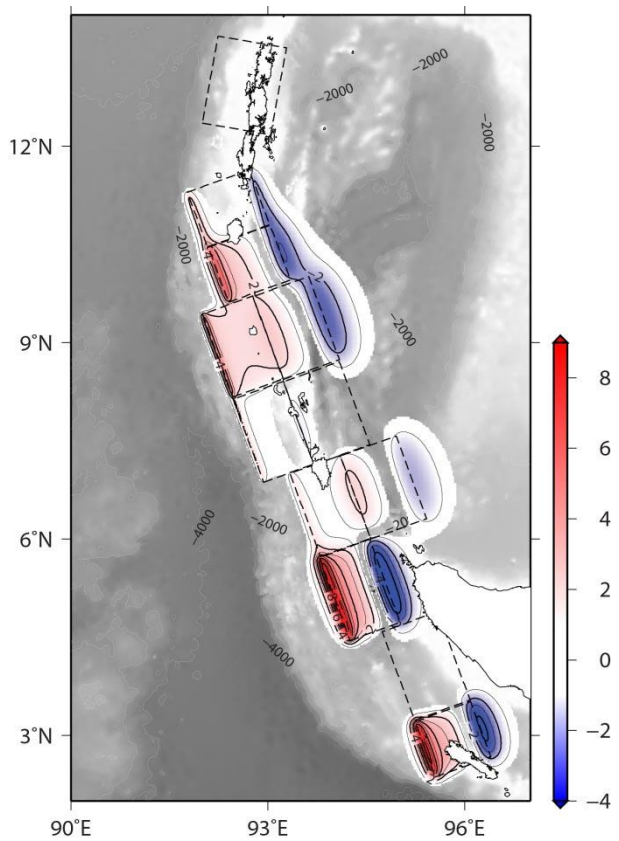

Figure 2. The vertical component of water deformation (meters) computed by Okada's solution

Figure 2 shows the total vertical component of water deformation computed using Okada's solution (1985). The initial elevation and velocity are assumed to be zero. The water deformation at each subfault is forced to additional water elevation in every time step during the rise time, assumed to be 2 minutes, of the tsunami wave from the rupture time. The water deformation (ΔU) is composed of the vertical displacement (Uz) and the vertical movement (Uh) converted by horizontal movement (Ux, Uy) at the bottom (H) slope.

$$\Delta U = Uz + Uh$$

$$Uh = -Ux\frac{\partial H}{\partial x} - Uy\frac{\partial H}{\partial y}$$

Table 1. Fault parameters of the Sumatra-Andaman Earthquake

Subfault	Latitude	Longitude	Length (km)	Width (km)	Depth (km)	Strike (degree)	Dip angle (degree)	Rupture time (min)	Slip (m)
A	2°22´N	95°33´E	100	100	10	340	10	0	21.1
B	3°14´N	95°14´E	160	100	10	340	10	1	0.0
C	4°27´N	94°15´E	150	90	10	340	10	1	22.9
D	5°44´N	93°48´E	150	90	10	340	10	3	4.2
E	6°00´N	94°34´E	150	100	27	340	10	3	9.6
F	6°52´N	92°56´E	150	90	5	340	10	5	5.1
G	7°08´N	93°42´E	150	100	22	340	10	5	0.0
H	8°10´N	92°28´E	150	90	5	340	10	7	11.2
I	8°26´N	93°14´E	150	100	22	340	10	7	13.9
J	9°37´N	92°24´E	100	110	10	340	10	8	14.5
K	10°27´N	92°05´E	100	110	10	340	3	10	7.3
L	12°21´N	92°00´E	150	115	5	10	17	12	1.1

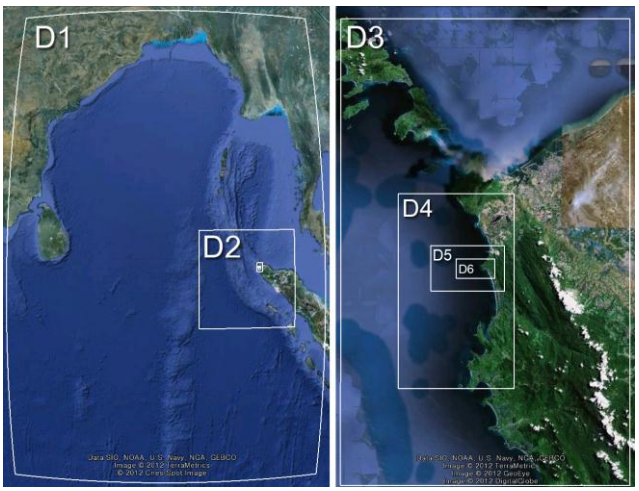

Figure 3. Domains of the tsunami propagation model

Table 2. Information on grid and nesting systems

Domain	NX	NY	DX DY (arc-sec)	DT (sec)	Nesting ratio	Comp Mode
D1	1000	1500	81	3		2D
D2	900	900	27	3	1:3	2D
D3	150	240	9	1	1:3	3D
D4	180	300	3	0.5	1:3	3Dwad
D5	345	210	1	0.1	1:3	3Dwad
D6	540	270	0.33	0.02	1:3	3Dwad

TSUNAMI PROPAGATION FROM SOURCE TO COAST

The tsunami propagation model has a multi-nesting system with a grid resolution from 2.5 km to 10 m, with the initial water elevation calculated using Okada's solution.

The finite difference Princeton Ocean Model (Mellor, 1998) was applied to simulate tsunami wave propagation during the 2004 Sumatra event. Six sub-regions, which all had different grid sizes, were used in the tsunami propagation model. The first and second domains (D1, D2) were computed in depth-averaged (2D) mode and the 3D mode was used for the third through sixth domains (D3–D6) with 10 vertical sigma levels. A radiation open-boundary scheme was used in the first domain (D1), and a one-way nesting scheme was used for the other domains by interpolating the water elevation and current values from the mother domain. The boundary condition of the internal model in the third domain (D3) employed the radiation scheme because the 3D current input was not available for the mother domain which was calculated in 2D mode.

Figure 3 shows the 6 domains of the numerical simulation with the one-way nesting system. The largest domain (D1) has a 1000 x 1500 mesh system with a grid resolution of 81 seconds (approximately 2.5 km) and a time step of 3 sec. The sub-domains are nested using 1:3 grid interpolations. The smallest domain (D6) has a 540 x 270 mesh system with a grid resolution of approximately 10 m and a time step of 0.02 sec. The "land" boundary conditions were assumed to be fully reflected in last sea grids from D1 to D3, with a minimum water depth of 10 m. The runup of tsunami waves in domains D4 to D6 was computed using the wet-and-dry scheme proposed by Oey (2005). The topography and bathymetry data are composed by GEBCO (Jones, 2003) and ASTER (Abrams et al., 1998) at 1 arc-second resolution. Because detailed topography data for the Lhok Nga hills is not available, various photographs from the survey reports and satellite images from Google Earth were used to modify the land elevation of the hills. Table 2 shows the information for the grid and nesting systems in all domains.

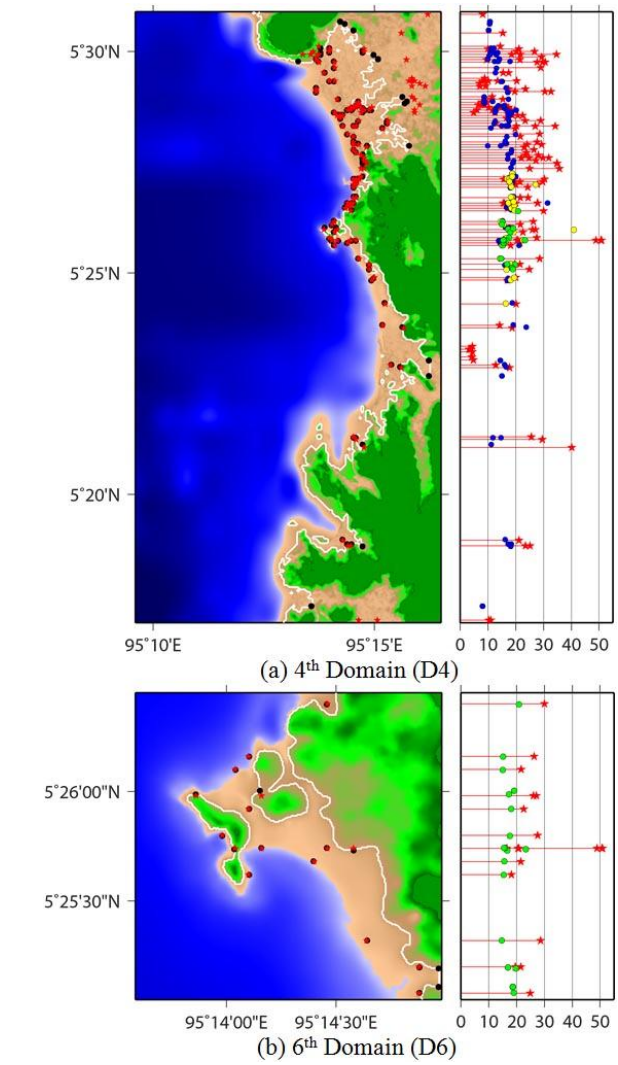

Figure 4. The figures on the left show the survey locations (red dots) and the locations of the closest computation points (black dots) for domains 4 and 6 by the tsunami propagation model. The figures on the right show the observed tsunami runup heights (red stars) and the computed runup heights (D4: blue dots, D5: yellow dots, D6: green dots)

The computed runup heights for domains 4 to 6 were compared with the observed heights in West Banda Aceh (Figure 4). The red dots in the figures on the left indicate the survey locations in the flooded areas, and the red stars in the figures on the right indicate the observed tsunami heights. The black dots in the figures on the left indicate the locations of the computed (wetted) grid points near the survey locations. The dots in the figures on the right indicate the computed maximum water elevations. The flooded area was estimated from the white contours, which indicate the boundary of the wetted computation grid.

The slight underestimates of the tsunami runup heights indicate that the numerical simulation results compare well with observed values for all coastal locations except the Lhok Nga Twin Peaks. However, the maximum tsunami runup height, over 50 meters, which was observed in the twin hills, cannot be reproduced by this model. Furthermore, due to the steep slopes of the hills, the vertical velocities are not small in comparison to the horizontal velocities, and non-hydrostatic effects should be considered significant. Tsunami behavior in such areas should be analyzed with fully nonlinear dispersive models. These phenomena have been observed for V-shaped valleys in the 1993 Hokkaido earthquake (Satake and Tanioka, 1995; Shuto and Matsutomi, 1995) and the 2011 East Japan earthquake (Tsuji et al., 2001).

TSUNAMI-INDUCED FLOW IN LHOK NGA TWIN PEAKS

To simulate the 3D wave field in the vicinity of Lhok Nga Twin Peaks with high accuracy, the Reynolds-averaged Navier–Stokes equations solved by the FLOW3D code (Hirt and Nichols, 1981; Flow Science, 2002) were used. FLOW3D uses a true volume-of-fluid (VOF) method to compute free surface motion and uses the fractional area/volume obstacle representation (FAVOR) technique to model complex geometric regions. A finite difference approximation is used for discretization of each equation. To describe turbulence in a viscous fluid, a version of the k-ε model, updated with the help of renormalization group analysis, is used (Yakhot and Orzag, 1986; Yakhot and Smith, 1992). This computer code has already been used to simulate tsunami waves (Choi et al., 2007, 2008a, b). Figure 5 shows the domain of the FLOW3D computation.

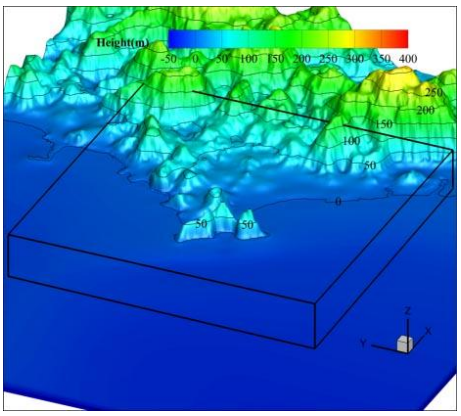

Figure 5. Model domain of Flow3D

It is quite difficult to apply boundary conditions in FLOW3D because this model accepts only single time-dependent boundary variables unless the code is customized. Thus, a representative boundary point was selected from the last domain of the POM model. This point has same center position at the west side of the FLOW3D domain. Figure 6 shows the water elevation and horizontal velocity used for boundary forcing. The surface elevation contains two large crests with amplitudes of 5 m following two large troughs with amplitudes of 8 and 12 m. Particle velocities in the tsunami waves were sufficiently large: approximately 4 m/s in both directions.

Numerical simulation makes it possible to reproduce the overflow of the tsunami waves between Labuhan Hill and Ritieng Hill. Figure 7 and Figure 8 illustrate this process. These figures clearly show that wave height is increased and reaches approximately 50 m and that water falls at a high velocity, up to 10 m/s.

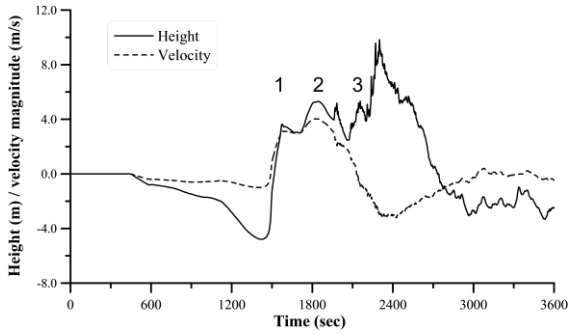

Figure 6. Water elevation and horizontal velocity used for boundary forcing in FLOW3D

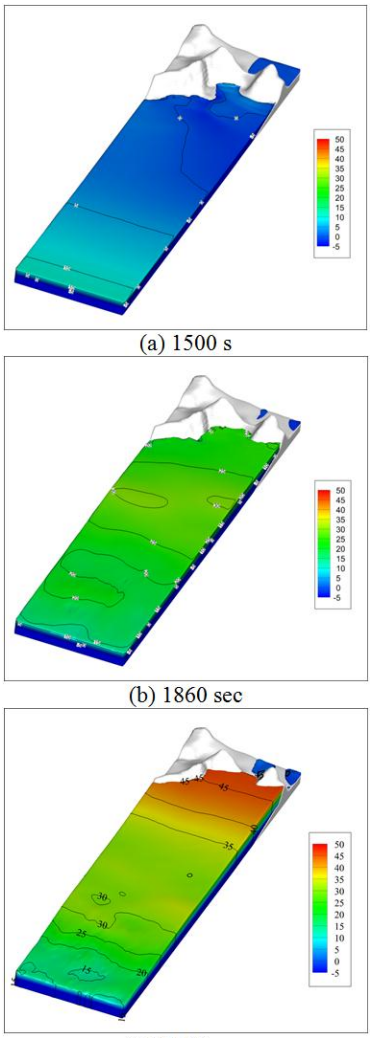

(a) 1500 s

(b) 1860 sec

(c) 2160 sec

Figure 7. Runup of waves computed by Flow3D in the west-east direction

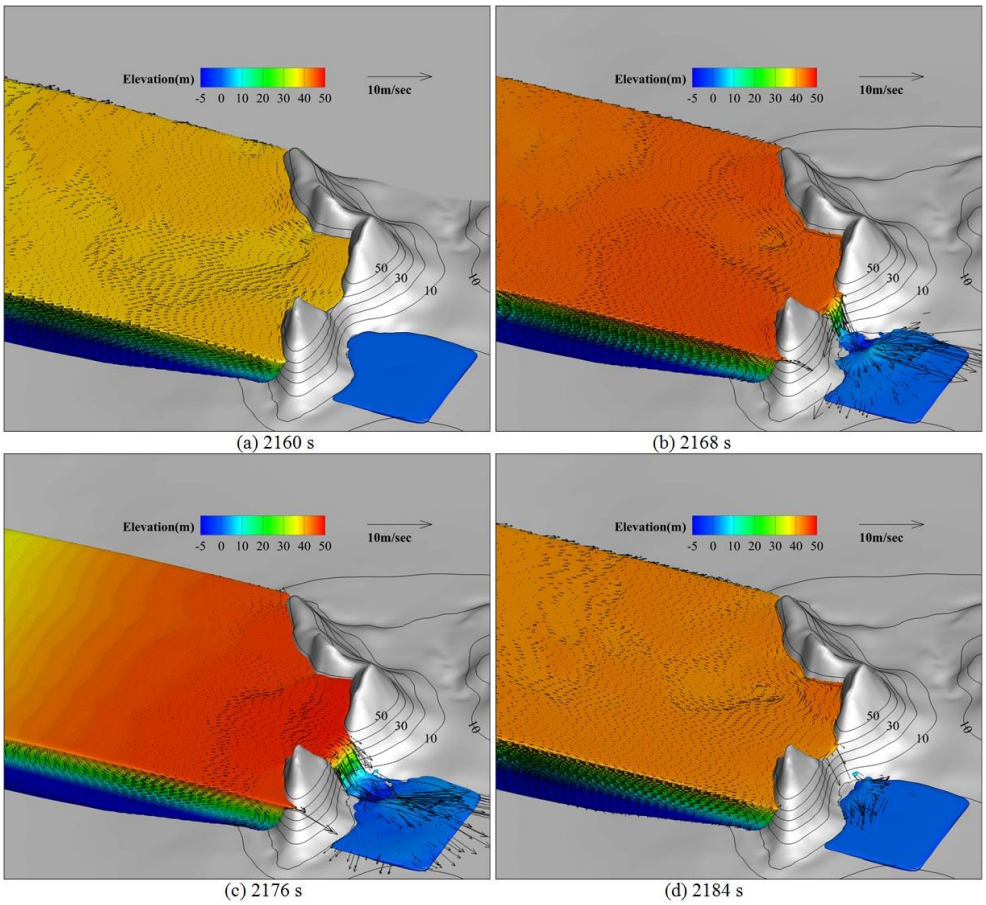

Figure 8. Overflow of tsunami waves through the saddleback between Labuhan Hill and Ritieng Hill.

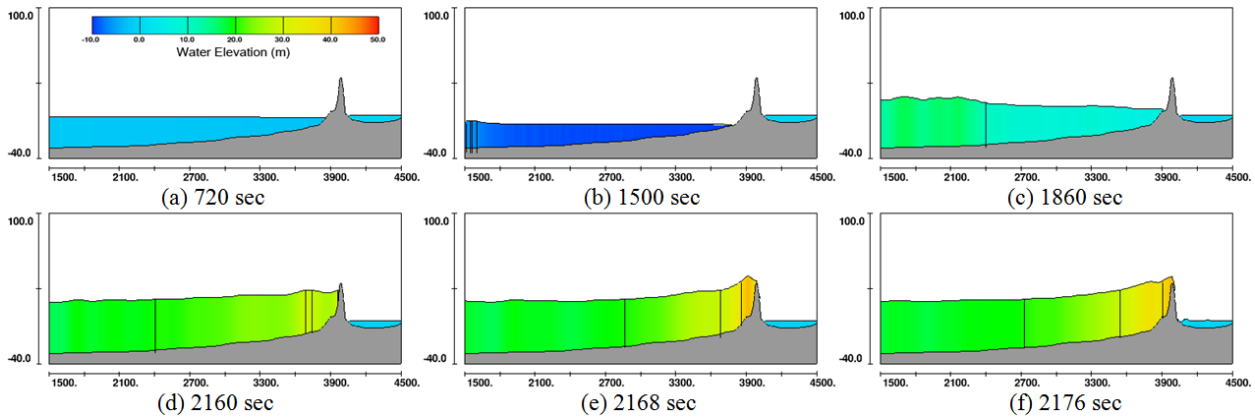

Figure 9. Snapshots of vertical profiles of the runup through the saddleback between Labuhan Hill and Ritieng Hill.

At 1500 sec after the occurrence of the tsunami (Figures 9b, 9c), the first tsunami wave reached the front of the twin hills, the wave height was approximately 13 m, and the tsunami wave was reflected and propagated from the twin hills to the sea. At 2160 sec after the occurrence of the tsunami (Figure 9d), the third tsunami wave reached the front of the twin hills, wave height was approximately 50 m or more, and overflow through the saddleback between the twin peaks occurred, as shown in Figures 8 and 9. Waves with steep fronts manifested as vertical tsunami waves were clearly observed flowing through the saddleback between Lubuhan Hill and Ritieng Hill.

CONCLUSIONS

The highest runup caused by the 2004 Sumatra–Andaman earthquake was recorded at the Leupung Beach twin peaks in Lhok Nga. The extreme runup height and overflow of the

saddleback between Labuhan Hill and Ritieng Hill was first reported by Shibayama at al. (2005) and was verified by Lavigne et al. (2009). A runup height of 51 m was measured on the saddleback between the hills. This is the highest recorded runup among the seismically generated tsunamis.

Simulation of the tsunami using a 3D hydrostatic finite difference model (POM) slightly underestimates the tsunami runup height, but otherwise yields results that compare quite well with observations for all coastal locations except the Lhok Nga Twin Peaks. The maximum tsunami runup height of over 50 m observed on the saddleback between the twin hills cannot be reproduced using the hydrostatic model. On the steepest slopes of the hills, the vertical velocities are not small in comparison to the horizontal velocities, and non-hydrostatic effects should be considered significant.

The coastal behavior of the tsunami at the Lhok Nga Twin Peaks was studied within the framework of fully nonlinear dispersive Reynolds-averaged Navier–Stokes equations using the FLOW3D code. The results clearly show that the wave height reached approximately 50 m and that water fell at velocities up to 10 m/s. The numerical simulation approach described in this paper makes it possible to reproduce the extreme characteristics of the tsunami in this coastal area, including the observed overflow through the saddleback between the twin peaks. Thus, 3D non-hydrostatic numerical models should be used in the future for prediction of tsunami characteristics on steep coasts and for estimation of tsunami risk for such areas.

ACKNOWLEDGEMENTS

This study was partially supported by the major research project “The development of the marine environmental impact prediction system following the disastrous event” funded by KIOST and by the BK21 Program at Sungkyunkwan University. EP has been particularly supported by Program “Scientific-Pedagogical Personnel of Innovative Russia for 2009-2013” and RFBR grant (11-05-00062).

LITERATURE CITED

Candella, R.N., Rabinovich, A.B. and Thomson. R.E., 2008. The 2004 Sumatra tsunami as recorded on the Atlantic coast of South America. *Advance in Geoscience*, 14, 117-128.

Choi, B.H., Kim, D.C., Pelinovsky, E. and Woo, S.B., 2007. Three-dimensional simulation of tsunami run-up around conical island. *Coastal Engineering*, 54, 618-629.

Choi, B.H., Pelinovsky, E., Kim, D.C., Didenkulova, I. and Woo, S.B., 2008a. Two- and three-dimensional computation of solitary wave runup on non-plane beach. *Nonlinear Processes in Geophysics*, 15, 489-502.

Choi B.H., Pelinovsky E., Kim D.C., Lee H.J., Min B.I. and Kim K.H., 2008b. Three-dimensional simulation of 1983 central East (Japan) Sea earthquake tsunami at the Imwon Port (Korea). *Ocean Engineering*, 35, 1545-1559.

Flow Science, 2002. FLOW-3D User's Manual.

Geist, E.L., Titov, V.V. and Synolakis, C. E., 2006. Tsunami: wave of change, *Scientific American*, 294, 56–63.

Hirt, C.W. and Nichols, B.D., 1981. Volume of fluid (VOF) method for the dynamics of free boundaries. *J. Comput. Phys.*, 39, 201-225.

Lavigne, F., Paris, R., Grancher, D., Wassmer, P., et al., 2009. Reconstruction of tsunami inland propagation on December 26, 2004 in Banda Aceh, Indonesia, through field investigations. *Pure and Applied Geophysics*, 166, 259-281.

Lay, T., Kanamori, H., Ammon, J.L. et al., 2005. The Great Sumatra-Andaman earthquake of 26 December 2004. *Science*, 308, 1127–1133.

Mellor, G.L., 1998. Users guide for a three-dimensional, primitive equation, numerical ocean model, Princeton University, NJ 08544-0710.

Merrifield, M.A., Firing, Y.L., Aarup, T. et al., 2005. Tide gage observations of the Indian Ocean tsunami, December 26, 2004. *Geophys. Res. Lett.*, 32, L09603.

Oey, L., 2005. A wetting and drying scheme for POM. *Ocean Modelling*, 9, 133-150.

Okada, Y., 1985. Surface deformation due to shear and tensile faults in a half-space. *Bull. Seismol. Soc. Am.*, 75, 1135-1154.

Paris, R., Wassmer, P., Sartohadi, J., Lavigne, F., et al., 2009. Tsunamis as geomorphic crises: lessons from the December 26, 2004 tsunami in Lhok Nga, West Banda Aceh (Sumatra, Indonesia). *Geomorphology*, 104, 59-72.

Poisson, B., Oliveros, C. and Pedreros, R, 2011. Is there a best source model of the Sumatra 2004 earthquake for simulating the consecutive tsunami? *Geophys, J. Int.*, 185, 1365-1378.

Rabinovich, A.B., Thomson, R.E. and Stephenson, F.E., 2006. The Sumatra Tsunami of 26 December 2004 as observed in the North Pacific and North Atlantic Oceans. *Surv. Geophys*., 27, 647–677.

Rabinovich, A.B. and Thomson, R.E., 2007. The 26 December 2004 Sumatra tsunami: Analysis of tide gauge data from the World Ocean. Part 1. Indian Ocean and South Africa. *Pure Appl. Geophys.*, 164, 261–308.

Satake, K. and Tanioka, Y., 1995. Tsunami Generation of the 1993 Hokkaido Nansei-Oki Earthquake. *Pure and applied geophysics*, 144, 803-821.

Satake, K., Okal, E. A., and Borrero, J. C., 2007. Tsunami and its hazard in the Indian and Pacific oceans: Introduction. *Pure Appl. Geophys.*, 164, 249–259.

Shibayama T., Okayasu, A., Sasaki, J., Suzuki, T., Matsumaru, Masimin, Atiff, Z., 2005. The December 26, 2004 Sumatra Earthquake Tsunami, Tsunami Field Survey in Banda Aceh of Indonesia, http://www.cvg.ynu.ac.jp/G2/indonesia_survey_ynu_e.html

Shuto, N. and Matsutomi, H., 1995. Field Survey of the 1993 Hokkaido Nansei-Oki Earthquake Tsunami. *Pure and applied geophysics*, 144, 649-663.

Tanioka, Y., Yudhicara, Kususose, T., Kathiroli, S., Nishimura, Y., Iwasaki, S. and Satake, K., 2006. Rupture process of the 2004 great Sumatra-Andaman earthquake estimated from tsunami waveforms. *Earth Planets Space*, 58, 203-209.

Thomson, R.E., Rabinovich, A.B. and Krassovski, M.V., 2007. Double jeopardy: Concurrent arrival of the 2004 Sumatra tsunami and storm-generated waves on the Atlantic coast of the United States and Canada. *Geophys. Res. Lett.*, 34, L15607.

Titov, V.V., Rabinovich, A.B., Mofjeld, H., Thomson, R.E. and Gonzalez, F.I., 2005. The global reach of the 26 December 2004 Sumatra tsunami. *Science*, 309, 2045–2048.

Tsuji, Y., Satake, K., Ishibe, T. Kusumoto, S., et al., 2011. Field Surveys of Tsunami Heights from the 2011 off the Pacific Coast of Tohoku, Japan Earthquake. *Bull. Earthquake Research Institute, University of Tokyo*, 86, 29-279 (in Japanese).

Yakhot, V. and Orszag, S.A., 1986. Renormalization group analysis of turbulence, I. Basic theory. *J. Scientific Computing*, 1, 1-51.

Yakhot, V. and Smith, L.M., 1992. The renormalization group, the expansion and derivation of turbulence models, *J. Scientific Computing*, 7, 35-61.